



Loss-of-stability vs yielding-type collapse mode in 3D steel structures under a column removal scenario: an analytical method of assessing the collapse mode

Panos Pantidis¹, Simos Gerasimidis²

Abstract

Progressive collapse of structures is the phenomenon of an initial failure mushrooming into global level, resulting in total or partial damage of the structure. This field is currently dominated by the Alternate Load Path Method, which involves the notion of a vertical key-component removal as the result of an abnormal event and the assessment of the remaining structure to bridge over the loss of that component. Previous work by the authors has shown that under a column removal scenario in a moment-resisting steel frame, the two most prominent collapse mechanisms are the loss-of-stability mode which involves the buckling of another column, and the yielding-type mode which is comprised by a series of plastic hinges at the beams ends and the eventual occurrence of a kinematic chain. The current paper expands this work in a 3D framework and develops a detailed numerical model of a 10story steel frame composite building. Interior gravity columns are removed along the height of the structure and the response of the structure in terms of the corresponding collapse mechanism is captured. The simulations are conducted using the finite element software ABAQUS and all the modeling assumptions are explicitly stated and discussed.

1. Introduction

Progressive collapse is a domino-type collapse mode of structures. It is usually triggered by an abnormal (or so-called extreme) event, such as an explosion, terrorist attack or even an extreme natural hazard, which is not considered in the design of the structure. The extreme event causes severe damage in a localized area of the structure, causing sudden changes in its stiffness and disturbing its equilibrium. Depending on the extent of the initial damage, the structure undergoes significant deformations trying to redistribute the already carried loads to the ground and to find a new equilibrium position. If an alternative load path is achieved, the impact of the extreme event is restricted in this area and damage does not spread out. However, if the structure lacks redundancy this new equilibrium position cannot be found and damage will propagate into an increasingly wider area, resulting in the collapse of a major part or even the whole of the structure.

¹ PhD Graduate Research Assistant, University of Massachusetts, Amherst, <ppantidis@umass.edu>

² Assistant Professor, University of Massachusetts, Amherst, <sgerasimidis@umass.edu>

There have been many reported progressive collapse incidents throughout the past decades. This phenomenon firstly attracted the attention of the scientific community after the Ronan Point Apartment collapse (London, 1968), where a gas explosion caused the elimination of two corner precast shear walls and subsequently the entire corner part of the building collapsed in a successive way. After the terrorist attacks in the Alfred P. Murrah Federal Building (Oklahoma, 1995) and particularly in the World's Trade Center (New York, 2001), research in this field was intensified and design guidelines were provided by the General Services Administration [1] and the Department of Defense (Unified Facilities Criteria – UFC) [2]. The design procedures included in these guidelines “aim to reduce the potential for progressive collapse by bridging over the loss of a structural element”. Among the design procedures proposed, the “Alternate Load Path Method” (APM) is most commonly employed. This is a threat-independent method, according to which a vertical, load bearing key-element is removed from the structural model and the capability of the remaining structure to redistribute the applied loads and find a alternative load path is assessed. In steel framed composite structures this key-element is usually a column. Among the available analysis methods, the “pushdown analysis” has been mainly adopted by researchers. According to the latter, once the structure has been modeled and the column has been removed, vertical downwards uniform load is applied to the model and it is incrementally increased from a zero value until a critical load value at which progressive collapse of the structure commences.

2. Preliminary work – Scope of the study

For the purposes of the present work the two most prominent collapse mechanisms that govern the behavior of a steel framed composite structure are termed as “yielding-type” and “stability” collapse mechanisms. The former is a complex mechanism. It depends on the geometric and material characteristics of the structure – it can involve some or all of the following phenomena: excessive deformations of the beam grillage and slab above the column removal (Fig. 1, maximum displacement denoted as “ δ ”), failure of beam connections, transition from flexure action into catenary action of the beams and rupture of the slab wire mesh reinforcement and metal deck. After rupture of the deck and the reinforcement, the slab is no longer capable of carrying the gravity loads. Significant research effort has been done towards this direction and important findings of numerical, analytical and experimental studies have been reported. Kwasniewski [3] developed a detailed finite element model of an 8-story building and studied its response under column removal scenarios, while Alashker et al. [4] employed 4 different numerical simulation approaches to explore the validity of certain modeling assumptions. Izzuddin et al. [5] proposed an analytical method to assess the robustness at various levels of structural idealization and Dinu et al. [6] conducted both an experimental analysis and numerical simulation of a two-way steel frame system subjected to a column removal scenario.

Since the loading domain of the structure at the moment of the column removal is dictated by downwards gravitational loads, stability plays a dominant role in the overall structural response. Instability phenomena may appear in a variety of ways, most common of which is the “short-wave instability”, expressed as column buckling. The increased axial demand of the columns in the vicinity of the column removal may exhaust the capacity of these columns. Additionally, due to the excessive deformations above the column removal a significant moment and horizontal

force is generated at these columns; the interaction among these internal forces and the axial demand may increase further the utilization ratio of the columns and push them beyond their design limit.

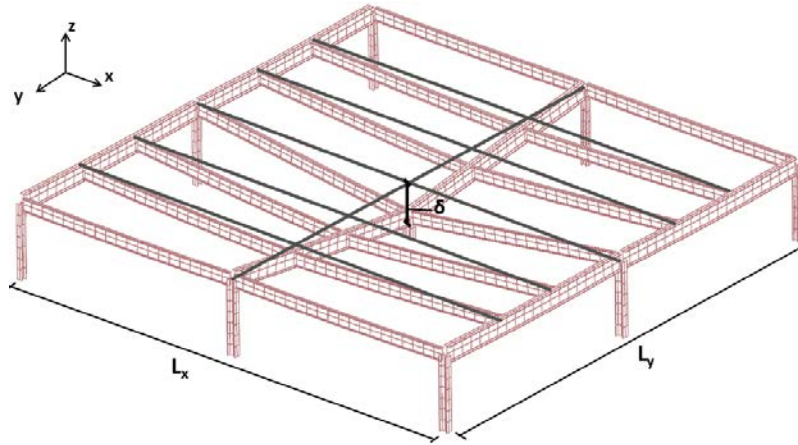


Figure 1: Typical beam grillage configuration above column removal

The difference among these two mechanisms is fundamental. In a ‘yielding-type case’ damage is mainly propagating “vertically”, so that damage largely affects the structural components around the column removal and at all floors above. It is a ductile mechanism, where energy is dissipated through excessive deformations of the structural components. In a stability-governed case however, damage is spreading out in a ‘horizontal’ way, triggering the columns to buckle one after the other. This is a very brittle collapse mechanism and takes place without prior warning, affecting at the same time the entirety of the building. The catastrophic nature of the second mechanism renders it highly undesired and necessitates the treatment of the building as a whole. This implies that the ductile beam-grillage design (to provide enough ductility and to resist the yielding-type collapse) should not drive damage propagation into columns, or in other words, the stability of the surrounding columns should always be ensured.

The main intention of this study is the investigation of the correlation between the location of the column removal and the corresponding collapse mechanism. In particular, the hypothesis that column removals in the lower part of the structure are associated with stability-governed collapse modes, while removals in the upper part trigger the yielding-type mechanism is examined. Gerasimidis [7] proposed a simple analytical method to distinguish these two collapse mechanisms in a 2D moment-resisting frame (MRF) subjected to an exterior column removal. Pantidis and Gerasimidis [8] refined the analytical method presented in [7] and conducted a parametric analysis of 120 2D MRFs with exterior column removal. Results revealed the clear distinction among the two mechanisms where stability governed the lower part of the structure and the yielding-type mode dominated the upper part. Gerasimidis and Sideri [9] developed a new partial distributed damage method (PPDM) to simulate damage distribution more realistically compared to the traditional single column removal scenario. According to this method damage is distributed in more than one columns and after investigating a variety of different scenarios the authors concluded that the APM may be unconservative in some cases. Gerasimidis et al. [10] examined the behavior of tall steel moment frame buildings under a ground floor column removal scenario. They demonstrated the existence of a global loss-of-

stability progressive collapse mechanism, where the frame loses its stability as a whole with very limited plasticity being developed prior to the occurrence of this global failure mode.

The current paper investigates numerically the progressive collapse mechanism of a prototype 10-story steel framed composite building. Using the finite element software ABAQUS [11], a three-dimensional model of the prototype building is generated and an interior gravity column is removed at each floor individually in-turn. Specific failure criteria are set in order to monitor the behavior and determine the initiation of each of the two collapse mechanisms. All the assumptions made are extensively discussed and justification of the modeling approach is provided.

3. Numerical simulation

3.1 Description of the prototype building

The examined building is extracted from the SAC-FEMA project [12] and corresponds to the 10-story Boston Pre-Northridge prototype building. Foley et al. [13] conducted an extensive study on the progressive collapse behavior of the three Boston Pre-Northridge buildings (3-story, 10-story and 20-story building) and provided additional information about these structures, especially regarding the secondary beams sections, the gravity columns orientation and the connections. Therefore the model used in the current paper aligns with the modifications-suggestions proposed in Foley et al. [13]. Fig. 2(a) shows the framing plan of the building. The structure has 4 perimeter MRFs to resist lateral loading and the connections denoted with filled triangle represent moment connections (rigid or fully restrained). Gravity columns, girders (in the y axis) and beams (in the x axis) are located in the interior of the building to resist the gravity load. The gravity system connections (denoted by a circle) are taken as flexible, implying that no moment is transferred to the columns. The building has a penthouse at the roof level and this region is enclosed by a dashed line. All column and beam members have an I-profile shape with their sections listed in Table 1. Spans in both directions share the same length of 9.144m. Fig. 2(b) shows a typical MRF of the structure. The first floor is below the ground and serves as the basement of the building. For the purposes of the current work this floor will be referred to as 'basement' and therefore the 1st floor is considered to be the one above the basement.

In order to perform a reliable progressive collapse analysis, the behavior of the connections needs to be carefully accounted for. Current guidelines ([1], [2]) provide modeling parameters and acceptance criteria for the connections which mainly rely upon seismic experimental data, where the loading scheme is fundamentally different from the one induced by a column removal scenario (cyclic horizontal load vs monotonic vertical load). In order to overcome these shortcomings several experiments of bare steel/composite connections subjected to axial force and/or bending moment/shear force have been conducted and simplified analytical models have been proposed, such as the one by Oosterhof and Driver [14]. However, since no simplified models more relevant to the particular loading domain have been universally accepted yet, the approach proposed in DoD [2] and particularly in Foley et al. [13] is adopted.

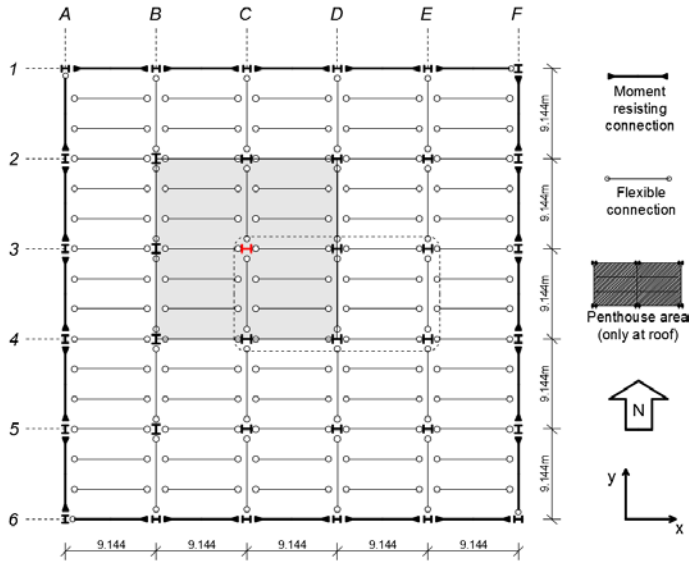


Figure 2(a): Framing plan of the prototype building

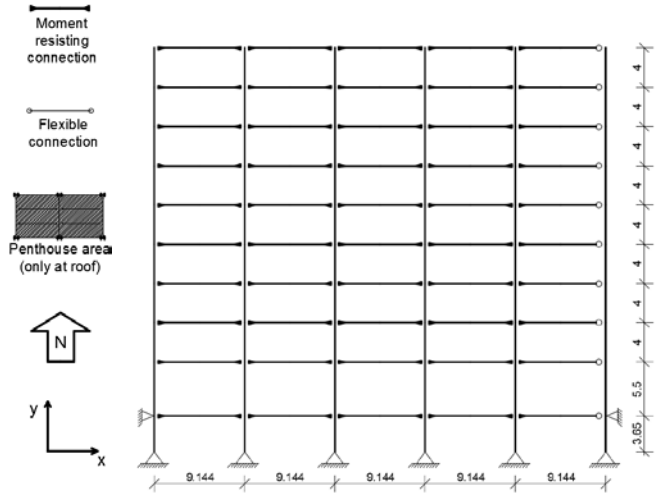


Figure 2(b): Typical MRF configuration

Regarding the shear connections of the gravity system, Foley [13] followed the subsequent approach:

1) A commonly used type of connection is assumed, namely the “double web angle” (bolted to both the beam web and the column flange). A variety of different geometries were developed (varying angle thicknesses, number of bolts) based on this connection type.

Table 1: Column and Beam Sections

Column Sections						Beam Sections			
Floor	A1, A6, F1, F6	A2-5, B1, B6, C1, C6, D1, D6, E1, E6, F2-5	B2-5, C2, C5, D2, D5, E2-5	C3, C4, E3, E4	D3, D4	MRF	Gravity		
						Floor	Section	Direction	Section
9 th	W14x61	W14x120	W8x48	W12x53	W12x58	Roof	W24x76	Along x (beams)	W18x35
7 th – 8 th	W14x90	W14x176	W12x65	W12x79	W12x79	9	W24x76		
5 th – 6 th	W4x132	W14x211	W12x96	W14x99	W12x106	8	W27x94		
						7	W30x99		
3 rd – 4 th	W14x159	W14x233	W12x120	W12x120	W14x132	6	W30x108	Along y (girder)	W24x68
1 st – 2 nd	W14x211	W14x283	W14x145	W14x145	W14x159	5	W30x116		
						4	W30x116		
						3	W33x118		
Basement	W14x211	W14x283	W14x176	W14x176	W14x176	2	W36x135		
						1	W24x76		

2) Based on the methodology of Shen and Astaneh-Asl [15] and Liu and Astaneh-Asl [16], a nonlinear tension and compression behavior relationship was developed for each bolt element accounting for the following limit states:

- a) Catenary tension fracture in the angle legs perpendicular to the beam web,
- b) Tear-out bearing failure of the bolts in the beam web,
- c) Tear-out bearing failure of the bolts in the angles,
- d) Tension fracture of the bolts including prying action (based on Thornton [17]),
- e) Shear fracture of the bolts.

3) Then, the pure tension, the pure moment and pure shear capacity and stiffness of the shear connection were determined, by assembling the results of step (2) for the total number of bolts and also accounting for two additional limit states (namely the “block shear rupture in the angle legs parallel to the beam web” and the “block shear rupture in the beam web”). This process was repeated for all the connection geometries generated from Step (1).

4) The progressive collapse analysis of the beam grillage was then performed, by assuming two equivalent springs replacing the connection. The first was an axial force-horizontal displacement spring and the second was a moment-rotation spring. The behavior of both springs was linear elastic until the maximum tensile force/moment and ‘perfectly plastic’ after that point, which is however an unconservative assumption. It is also important to note that Foley et al. [13] accounted for the moment capacity of the gravity connections, although these were assumed as rotationally pinned in the initial design of the prototype building.

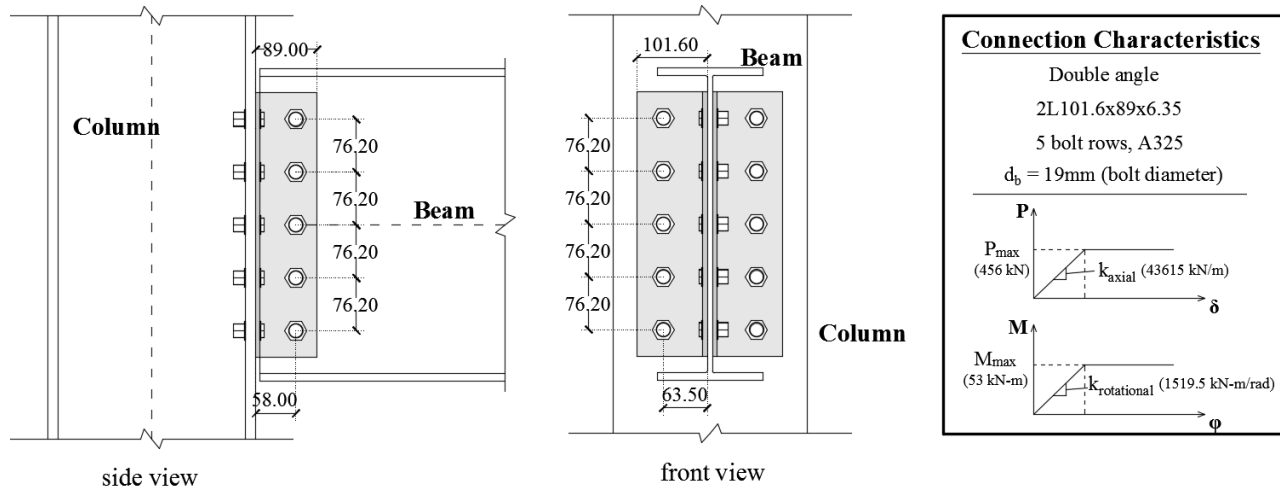


Figure 3: Geometric and Force/Moment characteristics of the assumed connection

More details of this approach can be found in Foley et al. [13]. For the purposes of the current study a specific connection geometry was assumed and its configuration is given in Fig. 3 (all length dimensions are in mm). This connection was taken for all the girder-to-column and the beam-to-girder shear connections of the model. According to Table 10-1 of AISC – Manual of Steel Construction [30] the W18x35 beam can support 3-5 bolt rows and the W24x68 beam can support 4-6 bolt rows. These values refer to “Simple Shear Connections” such as the ones

considered herein. The adopted connection is assumed to have 5 bolt rows. Foley et al. [13] studied the behavior of the 3-story Boston-Pre Northridge gravity system, which was comprised by W18x35 and W21x68 beams (instead of W24x68 as the 10-story). However, provided the fact that the W21x68 and the W24x68 beams have very similar dimensions and that for the given angle thickness the critical limit state was a double-angle limit state (“*Catenary tension fracture in the angle legs*”) and not a limit state dependent on the beam, the values of the maximum tensile force and moment given in Fig. 3 were extracted from Foley et al. [13] – Tables 6.4 & 6.5.

3.2 Description of the numerical approach

In this section an extended description of the numerical model is presented. All simulations were conducted using the finite element software ABAQUS/Standard. Beams and columns are modeled with the beam element B32OS, which is a 3D beam element with 2 interpolation points and an additional (7th) degree of freedom to account for the warping of the open section (13 section integration points were used). The appropriateness of this element to capture column buckling is evident in [4]. Reduced integration 4-point shell elements (S4R) with 5 integration points along the shell thickness are used to simulate the concrete slab. The slab is modeled sharing the same nodes with the beams (Fig. 4a) and through the “section assignment” option it is offset upwards at a certain distance, which corresponds to the distance between the slab bottom surface and the highest beam upper fiber (Fig. 4b). With this approach, full composite action between the beams and the slab is insured at any level of deformation. The centerlines of both the moment and gravity beams are assumed to be located in the same level. This assumption was also adopted in Li and El-Tawil [18] and its validity was examined. It was shown that it can play only a minor role at the first stages of the loading and that its importance was diminished in higher deformation levels such as the one induced by the current progressive collapse analysis.

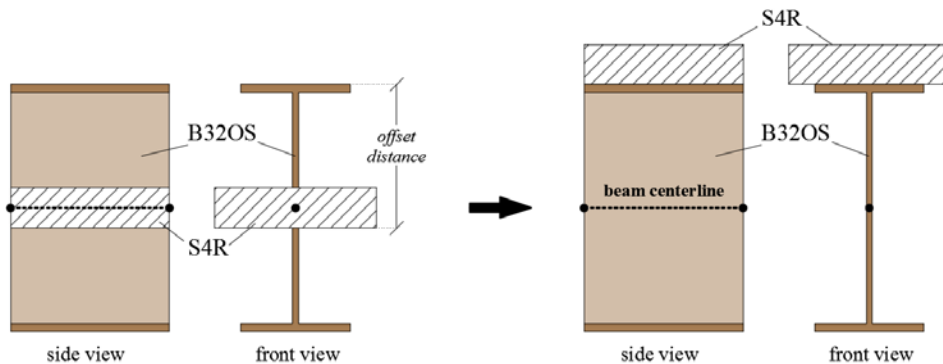


Figure 4(a): Slab and beam sharing same nodes

Figure 4(b): Slab offset to actual position

Material properties (modulus of elasticity, Poisson’s ratio, yield and ultimate stress, ultimate strain) of the steel used in the beams, the columns, the metal deck and the wire mesh reinforcement are provided in Table 2. The elastic behavior of the concrete slab is defined by a modulus of elasticity equal to 20GPa and a Poisson’s ratio equal to 0.2. Since no information regarding concrete was given in both SAC-FEMA [12] and Foley et al. [13], a compressive

stress of 20MPa was assumed for concrete. The “Concrete Damaged Plasticity” model of ABAQUS was chosen to define the inelastic concrete behavior, an approach also adopted in Agarwal and Varma [19], Liu et al. [20], Genikomsou and Polak [21], Vasdravellis et al. [22] and others. This model uses the yield function proposed by Lubliner et al. [23] and modified by Lee and Fenves [24] with a non-associated potential plastic flow. A value of 40° was chosen for the dilation angle and no significant changes were observed even using a lower value of 30° . The default values for the flow potential eccentricity ($\epsilon = 0.1$), the ratio of initial equibiaxial compressive yield stress to initial uniaxial compressive yield stress ($f_{b0} / f_{c0} = 1.16$) and the ratio of the second stress invariant on the tensile meridian to that on the compressive meridian ($k = 2/3$) were used. The viscoplastic regularization parameter which is used to improve to rate of convergence in regions of severe numerical difficulties was chosen as $5 \cdot 10^{-6}$. A parametric analysis was conducted for different values of the viscosity parameters (values ranging from 10^{-5} to 10^{-8}). No significant change was observed regarding the collapse mechanism and the corresponding vertical displacement above the column removal (the latter serves as the failure criterion of the yielding-type mechanism as it is further illustrated in Section 3.3). However the running time of each analysis was significantly higher for lower values than the chosen one, which led to the selection of this specific value. The tensile strength of the slab stems from the wire reinforcement and the metal deck (tension of concrete was neglected). The slab configuration provided in Foley et al. [13] was adopted. The slab has a thickness of 10cm and the contribution of the ribs was neglected.

Table 2: Structural Steel Properties

	Beams, Columns	Metal deck	Wire mesh reinforcement
E (KPa)	210000000		
v	0.3		
f_y (KPa)	345000	276000	448000
f_u (KPa)	448000	(perfectly plastic)	550000
ε_u	0.25	0.20	0.05

A 2VL122 steel deck is assumed and its tensile action is considered only across the direction of the flutes. As suggested in Alashker et al. [4] and Alashker and El-Tawil [25] only a portion of the deck yields at the maximum load with the value of the effective percentage ranging between 40% and 50% (50% taken in the current study). Its contribution was accounted through the “rebar layer” option in the “shell section” definition. Since the sub-beams are oriented in the E-W direction (Fig. 2) the deck was assumed to act in the N-S direction. 6x6 – W1.4xW1.4 wire mesh reinforcement is assumed, acting in both slab directions. Alashker et al. [4] used Eq. 1 to define an equivalent tensile stress-strain relationship for the slab (excluding the deck):

$$P_{t,eq}(\epsilon) = \frac{P_{t,R}(\epsilon) \cdot A_R}{A_{eq}} \quad (1)$$

where $P_{t,eq}(\varepsilon)$ is the equivalent tensile stress of the shell element at strain ε , A_{eq} is the equivalent area of the shell element per unit width, $P_{t,R}$ is the tensile stress of the wire mesh at strain ε and A_R is the area of the wire mesh per unit width. This approach is adopted in the current work and the tensile behavior of the concrete specified in the “Concrete Damaged Plasticity” model was based upon Eq. 1. Finally, as suggested in the Manual of Standard Practice of the Wire Reinforcement Institute [26], the fracture strain of the wire mesh reinforcement is taken as 0.05 (Table 3(c) - [26]). The rupture strain of the steel deck is taken as 0.20.

Moment (fully restrained) connections were inherently assumed by merging the nodes of the beams and columns converging at the same point. For the simulation of the shear connections of the gravity system the “connector elements” available from the ABAQUS element library were employed. Connector elements (or connectors) define a connection between a first and a second node by imposing kinematic constraints that make dependent (or optionally leave independent) the degrees of freedom (DOFs) of the second node to the DOFs of the first node. They essentially act as “springs” in a sense that the user can specify the relative displacements and rotations of the two nodes (they are referred to as “components of relative motion”), once a local axis system has been specified. The “Slot + Rotation” type of connector was used and Fig. 5 shows a representative example of this connector element, the orientation of the axes and the values assigned to the components of relative motion. The term “rigid” in Fig. 5 implies that the DOF of the second node is constrained to the DOF of the first node.

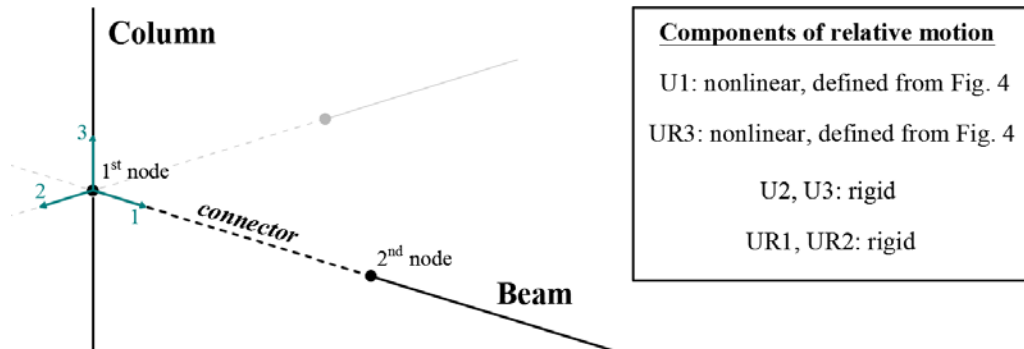


Figure 5: Connector element modeling

The nonlinear relationships for the components of relative motion U1 and UR3 are defined as specified from Fig. 4 and the connection is assumed to be fully restrained with regard to bending around the minor and twisting around the longitudinal axis.

The base nodes of the model are assumed to be pinned. Since the basement is below the ground, all the translational DOFs at the level of the ground floor are restrained (Fig. 2). A pushdown analysis which accounted for both material and geometric nonlinearities was conducted. An arbitrary uniform, vertical, downwards load of 50KPa was applied in all floors except the roof, where it was replaced by a load of 40KPa (SAC-FEMA [12], Foley et al. [13]). Since the interest of this study lies in the behavior of a typical 3D structure under a progressive collapse scenario, the penthouse load was excluded from the calculations to insure symmetric loading of the

building. The load increment had an initial and maximum value of 0.005 and minimum value of 10^{-7} , to insure that the load was applied as slowly as required to capture accurately the nonlinear behavior of all structural components. Loading started from a zero value and it was increased incrementally until some of the failure criteria set in Section 3.3 were met. According to DoD [2], when a nonlinear static analysis is employed the gravitational load applied in the area above the column removal (shaded area of Fig. 2) has to be multiplied by the dynamic increase factor Ω_N to account for the dynamic nature of the phenomenon. For steel framed buildings this factor is calculated according to Eq. 2:

$$\Omega_N = 1.08 + \frac{0.76}{(\theta_{pra} / \theta_y) + 0.83} \quad (2)$$

θ_y is the beam yield rotation and it is defined in Eq.3 (ASCE 41 – Equation 5-1 [27]):

$$\theta_y = \frac{W_{pl} \cdot f_y \cdot L}{6 \cdot E \cdot I} \quad (3)$$

where W_{pl} is the plastic modulus, f_y is the yield stress, l is the length of the beam, E is the modulus of elasticity and I is the moment of inertia. θ_{pra} is the plastic rotation angle and contrary to θ_y it refers to the connection. Table 5-2 of DoD [2] defines the following relationships for θ_{pra} when the connection is flexible, double angle and the limit state is flexure in angles (as herein):

$$\theta_{pra} = 0.1125 - 0.0027 \cdot d_{bg} \quad (4)$$

$$\theta_{pra} = 0.15 - 0.0036 \cdot d_{bg} \quad (5)$$

for primary and secondary components respectively, where d_{bg} is the depth of the bolt group in inches and θ_{pra} is given in radians. The process for the calculation of Ω_N is given in Table 3. Two important notes have to be made here. Firstly, according to DoD [2] this particular connection type has a significantly ductile behavior which results in high values of θ_{pra} and eventually low values of Ω_N . If a more brittle limit state was the critical one (bolt failure in shear or tension) the value of Ω_N would be approximately 1.273. Secondly, a perfectly plastic behavior of the connection is assumed by DoD [2], which was also adopted in Foley's study [13]; however the assumed behavior is based upon connection performance under earthquake loading and a different behavior should be expected under monotonic gravity loading combined with significant axial force in the connections.

Table 3: Dynamic Increase Factor calculation

Beam	Component	W_{pl} (m^3)	I (m^4)	L (m)	f_y (MPa)	E (GPa)	d_{bg} (m)	θ_y	θ_{pra}	Ω_N
W18x35	Secondary	0.00109	0.0002123	9.144	345	210	0.3048	0.0129	0.107	1.163
W24x68	Primary	0.0029	0.0007617	9.144	345	210	0.3048	0.00953	0.08	1.162

3.3 Failure criteria

Specific failure criteria are set for each of the two collapse modes. Column buckling (indicating the stability failure) is numerically met when the axial demand of the column approaches the inelastic critical buckling load of the column, in conjunction with an excessive and abrupt increase in the horizontal displacement of the column middle point. Additionally, the von Mises stresses are in accordance with the inelastic column buckling theory (Shanley [28]) and negative eigenvalue messages appear in the ABAQUS message file, implying singularities in the stiffness matrix. Given the unconservative assumption regarding the post-peak behavior of the connections where a ‘perfectly plastic’ behavior is assumed, the yielding-type mechanism is assumed to initiate when the vertical displacement δ above the column removal reaches half of the critical value identified by Alashker and El-Tawil [25] and Park [29]. They have defined their failure criteria when δ is of 10% of the shortest span length, while the present study assumes 5%.

3.4 Results and Discussion

The interior gravity column located at C3 (shown with red color in Fig. 2) is removed from the model at each floor individually in-turn (1st to 9th). The results are comprehensively presented in Table 4. The first column refers to the column removal scenario analyzed. The second column indicates the observed collapse mechanism when the failure criteria set in Section 3.3 were met – in the case of the stability mode the location of the buckled column is also depicted. The third column displays the corresponding maximum vertical displacement of the beam grillage above the removed column and the fourth column depicts the applied load at the onset of collapse

The first observation regarding the results of Table 4 is that the stability failure mechanism can indeed govern the behavior of the building in some column removal cases. It was evident from the results that “catenary action” was not capable to form prior to the column buckling. This is considered a very important finding and it opens the discussion over the appropriateness of reduced models that are commonly employed in a progressive collapse analysis. Since they inherently exclude the columns, stability phenomena are consequently not studied. Reduced models can indeed be very efficient when a column removal scenario in the upper part of the structure is analyzed; yet extreme caution should be paid before generalizing their outcome and postulating a conclusion about the behavior of the entire building.

Table 4: Analysis results

Column Removal	Collapse mechanism	Max. displacement (m)	Collapse load (KPa)
1 st	Buckling (B3 - 1st floor)	0.631	8.40
2 nd	Buckling (B3 - 2nd / 3rd floor)	0.726	9.03
3 rd	Buckling (B3 - 3rd floor)	0.729	9.00
4 th	Buckling (B3 - 4th floor)	0.825	9.65
5 th	<i>Simultaneous</i>	0.903	10.10
6 th	Yielding	0.914	10.15
7 th	Yielding	0.914	10.15
8 th	Yielding	0.914	10.35
9 th	Yielding	0.914	11.50

The second comment which can be made is that there is indeed a switch from the brittle, stability progressive collapse mode to the ductile, yielding-type mode as the column is removed from the bottom part towards the upper. This observation aligns with the results of Pantidis and Gerasimidis [4] and further validates the hypothesis that column removal scenarios in different regions of the building can cause fundamentally different structural response. This finding leads to the conclusion that each column has a different effect on the overall structural behavior, which further confirms the notion that generalizing the results of a specific column removal scenario to the entire building progressive collapse behavior is not always applicable.

Another important note is that the load at which the collapse mechanism is triggered decreases as we move to the bottom part of the structure. This finding clearly shows that under the actual gravity loads of the real structure, progressive collapse is more possible to occur when a column that belongs to the lower part is removed – a scenario which has a high probability to trigger the stability mode. Therefore simulating a column removal scenario at the upper part of the structure is considered to be an unconservative approach if the overall structural behavior is sought.

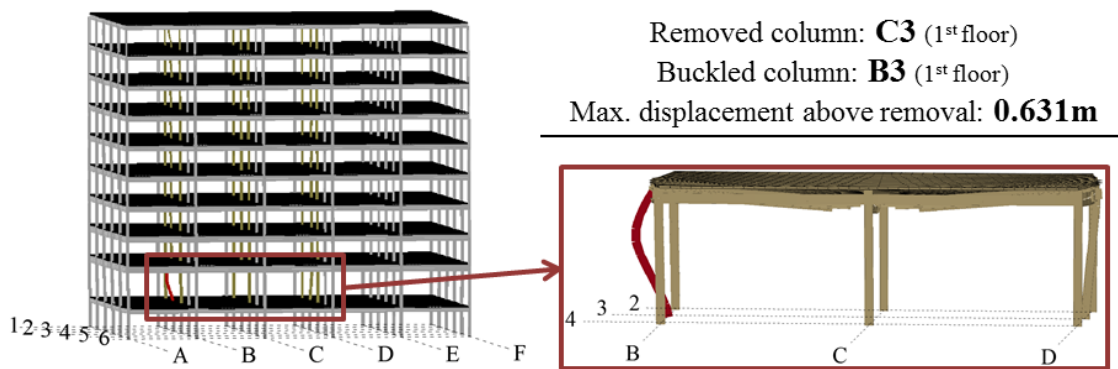


Figure 6: Deformed shape of structure – 1st floor column removal scenario

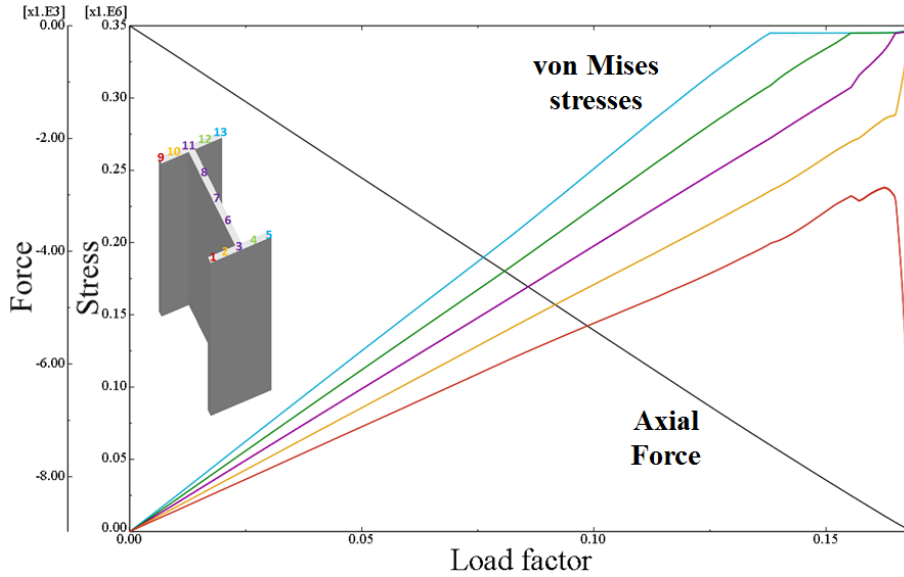


Figure 7: Axial force and von Mises stresses of the buckled column B3 – 1st floor column removal scenario

Fig. 6 shows a typical example of the stability case, namely the removal at the 1st floor. The deformed shape of the entire structure with a detailed picture of the region of the buckled column is depicted (the column buckles around the weak axis). The deformation scaling factor along the x-axis has a value of 40 in order to achieve higher clarity and to clearly present the final position of the buckled column. Fig. 7 depicts the evolution of the axial force (black line) and the von Mises stresses of the buckled column. The axial force reaches a maximum value of $P_{\max, \text{demand}} = 8927 \text{ kN}$, whereas the inelastic buckling capacity is $P_{\text{inelastic}} = f_y * A = 9500 \text{ kN}$. The column buckles before it reaches this value and this is due to the interaction of the axial load and the bending moment. The presence of the latter is apparent in the von Mises stresses diagram where section points 1, 9 and 5, 13 are subjected to significantly different compressive stresses. This finding validates the hypothesis that the interaction of the bending moment and the axial load will cause the column to buckle before it reaches the purely compressional inelastic buckling load. Finally, Fig. 8 shows the deformed shape of the structure in a typical example of the “yielding” type collapse, namely the removal at the 7th floor, where the displacement reaches the value of 0.914m (failure criterion in Section 3.3).

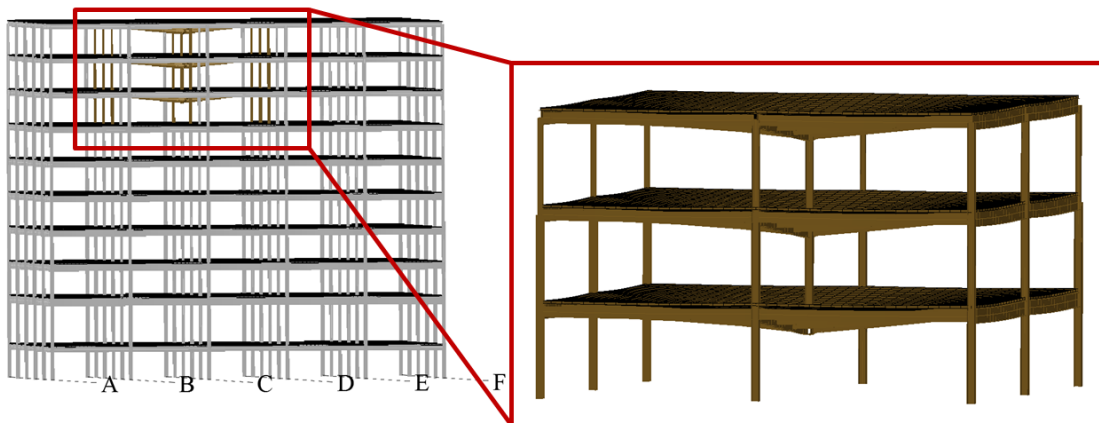


Figure 8: Deformed shape of structure – 7th floor column removal scenario

3.5 Alternative connection approaches – preliminary results

In this section the preliminary results of a brief parametric study regarding the connections are reported. Two additional column removal analyses with modified connection behavior are conducted, deviating from the assumptions by Foley et al. [13].

In the first analysis the rotational capacity of the connections is neglected and only the axial load-displacement spring is considered. This choice is justified by the fact that the connections in the initial design of the structure are assumed to be flexible and to have negligible moment capacity and stiffness. A column removal scenario in the first floor was analyzed. The results indicated that although the maximum vertical displacement above the removal was increased and reached a value of 0.729m (contrary to the 0.631m displacement observed when the connection moment capacity had been taken into account), the collapse mechanism was again buckling of column B3 at approximately the same collapse load value (8.50 KPa).

The second modification regarded the number of the connection bolt rows. Foley et al. [13] suggested that the axial connection capacities should be on the order of $0.2P_y - 0.3P_y$, where $P_y = A * f_y$ is the beam axial capacity. It was also stated that better levels of structural integrity can be achieved when the maximum number of bolt rows that the beam or girder can support is utilized (namely 5 bolt rows for the W18x35 beam and 6 bolt rows for the W24x68 girder, as it was described in Section 3.1). For the second analysis a conservative connection geometry was assumed. According to Table 10-1 of AISC – Manual of Steel Construction [30] for “Simple Shear Connections” the minimum number of bolt rows that a beam can support is 3 for the W18x35 and 4 for the W24x68 beam. According to Foley et al. [13], this number of bolts corresponds to an axial capacity of 274 KN ($0.12P_y$) and 365KN ($0.08P_y$) respectively, when the minimum angle thickness ($t = 6.35\text{mm}$) is used. For this connection geometry and neglecting at the same time the connection moment capacity, a 1st floor column removal analysis was conducted. The tip vertical displacement had just approached the value of 0.9m when column B3 buckled at a load value of 8.50KPa. The latter finding reveals that even with very conservative connection modeling assumptions, where the connections are assumed to have a) the minimum angle thickness, b) no moment capacity and c) an axial capacity of approximately only 10% of the corresponding beam, a column removal scenario at the bottom part of the structure triggers the stability collapse mechanism.

3.5 Limitations and ongoing research

It has to be explicitly stated here that these specific results are the outcome of the aforementioned modeling assumptions. These assumptions were made on the basis of previous published research of the authors, other researchers’ work or current guidelines. However, no experimental validation of the results has been done on this extent of structures. Therefore, the intention of the authors is not to provide a strict statement over the progressive collapse behavior of this specific prototype building but to point out the existence and importance of the stability collapse mechanism. The main assumption that requires further investigation is the behavior of the connections. In particular the “perfectly plastic” behavior of both the axial load-displacement and the moment-rotation relationships of the equivalent springs is questionable and it is thought

to be unconservative. Ongoing research of the authors is currently focusing in a more realistic representation of the connections, in terms of their actual behavior under the combination of gravity load and significant horizontal forces.

The aim of the authors is the development of an analytical solution to describe the progressive collapse behavior of a 3D structure and ongoing research is also focusing towards this direction. An approach similar to Pantidis and Gerasimidis [4] will be adopted. Closed form expressions that will provide the collapse load value of each of the two mechanisms for a given column loss scenario will be derived. These expressions will be based only on the geometric and material characteristics of the building and they will be functions of the position of the column removal, in order to provide a general analytical solution for any column removal scenario that the structure may undergo. These results will be then assembled and expressed through the notion of the Euler-type curves, which is essentially the graphical representation of the collapse mechanism as a function of the column removal location (more details can be found in Pantidis and Gerasimidis [4]).

4. Conclusions

A prototype 10-story steel framed composite building is subjected to 9 interior gravity column removal scenarios along its height and its structural response is investigated using powerful finite element analysis software. All the primary structural components were modeled, either directly (beams, columns, slab, connections) or indirectly (wire reinforcement, deck). All the modeling assumptions are explicitly stated and justification for their adoption is provided at each step. The results indicate the existence of two progressive collapse modes: a) the stability mode which governs the behavior for the 1st – 4th column loss scenarios and b) the “yielding-type” mode which dominates the behavior for the 6th – 9th column removal cases (the two mechanisms are triggered almost simultaneously when the gravity column of the 5th floor is removed). These findings clearly demonstrate that the structural behavior assessment under a column loss scenario requires the consideration of the entire building and not just a part of it, in order to numerically capture all the phenomena that may appear. Since the connections are the first structural components to be affected and their response greatly affects the structure’s behavior, current work by the authors is primarily focused on more realistic connection modeling and correct assessment of their impact on the corresponding collapse mode.

References

- [1] US General Service Administration (GSA); 2013. “Alternate path analysis & design guidelines for progressive collapse resistance”.
- [2] DoD (2009). Unified Facilities Criteria (UFC), “Design of buildings to resist progressive collapse”. Washington, DC: Department of Defense
- [3] Kwasniewski, L. (2010). “Nonlinear dynamic simulations of progressive collapse for a multistory building”, *Engineering Structures*, 32: 1223-1235
- [4] Alashker, Y., Li, H., El-Tawil, S. (2011). “Approximations in progressive collapse modeling”, *Journal of Structural Engineering*, 137: 914-924
- [5] Izzuddin, B.A., Vlassis, A.G., Elghazouli, A.Y., Nethercot, D.A. (2007). “Progressive collapse of multi-storey buildings due to sudden column loss-Part I: Simplified assessment framework”, *Engineering Structures*, 30: 1308-1318

- [6] Dinu, F., Marginean, I., Dubina, D., Petran, I. (2016). "Experimental testing and numerical analysis of 3D steel frame system under column loss", *Engineering Structures*, 113: 59-70
- [7] Gerasimidis, S. (2014). "Analytical assessment of steel frames progressive collapse vulnerability to corner column loss", *Journal of Constructional Steel Research*, 95: 1-9
- [8] Pantidis, P., Gerasimidis, S. (2016). "New Euler-type progressive collapse curves for steel frames", *Proceedings of the Annual Stability Conference*, Structural Stability Research Council, Orlando, Nashville
- [9] Gerasimidis, S., Sideri, J. (2016). "A new partial-distributed damage method for progressive collapse analysis of steel frames", *Journal of Constructional Steel Research*, 119: 233-245
- [10] Gerasimidis, S., Deodatis, G., Yan, Y., Ettouney, M. (2016). "Global instability induced failure of tall steel moment frame buildings", *Journal of Performance of Constructed Facilities*, 04016082
- [11] Simulia (2012). ABAQUS theory manual, version 6.12, Providence, RI: Dassault Systems Corporation
- [12] FEMA-355C (2000). State of the art report on systems performance of steel moment frames subject to earthquake ground shaking, Washington DC: Federal Emergency Management Agency
- [13] Foley, C., Martin, K., Schneeman, C. (2007). "Robustness in structural steel framing systems", *Final Report submitted to American Institute of Steel Construction, Inc.* Chicago, IL
- [14] Oosterhof, S., Driver, G. (2016). "Shear connection modelling for column removal analysis", *Journal of Constructional Steel Research*, 117: 227-242
- [15] Shen, J., Astaneh-Asl, A. (2000). "Hysteresis model of bolted-angle connections", *Journal of Constructional Steel Research*, 54: 317-343
- [16] Liu, J., Astaneh-Asl, A. (2000). "Cyclic testing of simple connections including effects of slab", *Journal of Structural Engineering*, 126(1): 32-39
- [17] Thornton, W.A. (1985). "Prying action – A general treatment", *Engineering Journal*, Second Quarter, American Institute of Steel Construction, Chicago, IL, 67-75
- [18] Li, H., El-Tawil, S. (2014). "Three-dimensional effects and collapse resistance mechanisms in steel frame buildings", *Journal of Structural Engineering*, 140
- [19] Agarwal, A., Varma, A.H. (2014). "Fire induced progressive collapse of steel building structures: the role of interior gravity columns", *Engineering Structures*, 58: 129-140
- [20] Liu, J., Tian, Y., Orton, S.L. (2015). "Resistance of flat-plate buildings against progressive collapse. I: modeling of slab-column connections", *Journal of Structural Engineering*, 141(12): 04015053
- [21] Genikomsou, A., Polak, M.A. (2015). "Finite element analysis of punching shear of concrete slabs using damaged plasticity model in ABAQUS", *Engineering Structures*, 98: 38-48
- [22] Vasdravellis, G., Uy, B., Tan, E.L., Kirkland, B. (2012). "Behavior and design of composite beams subjected to negative bending and compression", *Journal of Constructional Steel Research*, 79: 34-47
- [23] Lubliner, J., Oller, S., Onate, E. (1989). "A plastic-damage model for concrete", *International Journal of Solids and Structures*, 25: 299-326
- [24] Lee, J., Fenves, G.L. (1998). "Plastic-damage model for cyclic loading of concrete structures", *Journal of Engineering Mechanics*, 124:8(892) 892-900
- [25] Alashker, Y., El-Tawil, S. (2011). "A design-oriented model for the collapse resistance of composite floors subjected to column loss", *Journal of Constructional Steel Research*, 67: 84-92
- [26] Wire Reinforcement Institute (2006). "Manual of standard practice – structural welded wire reinforcement",
- [27] American Society of Civil Engineers ACE/SEI 41-06. (2007). "Seismic rehabilitation of existing buildings"
- [28] Shanley, F.R. (1947). "Inelastic Column Theory", *Journal of Aeronautical Science*, 14(5), May: 261
- [29] Park, R. (1964). "Tensile membrane behavior of uniformly loaded rectangular reinforced concrete slabs with fully restrained edges", *Magazine of Concrete Research*, 16(46), London, ENG, 39-44
- [30] AISC (2014). "Manual of Steel Construction", American Institute of Steel Construction, Chicago, IL